ALD Oxides-Based *n-i-p* Heterostructure Light Emitting Diodes

S. Gieraltowska*, L. Wachnicki and M. Godlewski
Institute of Physics, Polish Academy of Sciences, Aleja Lotnikow 32/46, PL-02668 Warsaw, Poland

(Received July 27, 2018)

The aim of this work was an analysis of structural, electrical and optical properties of n-type ZnO/i/p-type (called as n-i-p) GaN heterostructure with interlayer between these semiconductors. Such junctions are promising structures for light-emitting diodes, light detectors in the range of ultraviolet radiation and photovoltaic cells. This work concentrates on the investigation of the influence of oxide interlayers in optoelectronic structures, and optimization of growth parameters (in the atomic layer deposition — ALD process) of all oxide layers. Composition of HfO_2, TiO_2, ZrO_2 and Al_2O_3 films was also optimized. The layers were used as intrinsic barriers to improve the performance and realize color shift of the n-ZnO/p-GaN heterojunction LEDs. The rectification ratio of n-i-p junctions was $I_{on}/I_{off} = 1 \times 10^2$–$10^3$ for the voltage of 20 V. The color emission of these devices was adjusted from violet to white light in a room temperature depending on the growth parameters and composition of the ALD oxide layers.

DOI: 10.12693/APhysPolA.134.596
PACS/topics: 79.60.Jv, 73.40.Lq, 81.15.–z

1. Introduction

Light emitting diode (LED) technology is currently intensively developing, because in the near future, efficient, low-energy LEDs will become one of the primary light sources used in lighting [1]. In comparison with the standard light sources, LEDs are more energy efficient, and therefore are more economical [2].

After the breakthrough in stable p-doping, gallium nitride (GaN) material is attracting tremendous interest for GaN-based short wavelength optoelectronic devices, such as blue light-emitting diode, solid ultraviolet detector, and laser diode [3, 4]. Although, high-power p-n homojunction blue-LEDs have been fabricated with commercial success using p-GaN/n-GaN homostructures with the 430 nm main electroluminescence (EL) peak, they require further improvement [5]. Zinc oxide (ZnO) seems to become the next focus of research after GaN in wide band gap semiconductor materials. The main challenge in ZnO is p-type doping [6]. Although much progress has been made in this area, the fabrication of effective ZnO-based LEDs and laser diodes still must await further development of good, reproducible, p-type material [7]. Due to these difficulties, it has been reported that the n-ZnO/p-ZnO homostructures show very weak electroluminescence [8]. Based on similar properties of ZnO and GaN materials, and the relative availability and stability of good quality p-GaN and n-ZnO, the production and acting of heterostructures combining n-ZnO with p-GaN has been reported previously in literature [9, 10]. These wide-band-gap semiconductors have been proposed by virtue of their similarity in crystalline wurtzite structure with lattice constant mismatch about 1.6% and similar band gaps in room temperature (≈ 3.4 eV) [6]. Further advantage of n-ZnO/p-GaN LEDs is that heterojunction-based devices exhibit improved current confinement compared to n-GaN/p-GaN, which leads to higher recombination and improved device efficiency. Similar physical properties of ZnO and GaN allow creation of LEDs emitting in a short wavelength spectral region. However, their heterostructures LEDs with the EL in the blue-violet region (with peak wavelength in the range of 400–430 nm) emit mainly from the p-GaN instead of the n-ZnO, by reason that the electron injection from n-ZnO would reign over the hole injection from p-GaN due to the higher carrier concentration in n-ZnO [11, 12]. Despite that fact, ZnO could exhibit all the colors emission in the visible range related to deep level emission bands therefore it is even recognized as a promising candidate material for the optoelectronic industry [13]. This opens the possibility to use them as materials for a n-p junctions for applications in optoelectronic devices.

In this letter, we reported on the growth and device properties of modifying the n-p heterojunctions with high-k oxide layers (interlayer, intrinsic layer) with a wide-band-gap inserted between the semiconductor layers. The creation of the n-ZnO/i/p-GaN improved the performance, stability, and changed the range of light emission. The major reason of an introducing of these intrinsic layers separating n-ZnO and p-GaN was related to charge carriers flow through the junction [14, 15]. The oxide films were obtained using the ALD system at low temperature (well below 300 °C) on p-type magnesium doped GaN templates. It proved that the low growth temperature regime was crucial for obtaining high-k oxides (HfO_2, TiO_2, Al_2O_3, ZrO_2) and n-conductivity ZnO, at least in case the ALD growth was referred [16–18]. This method enabled excellent thickness control of thin

*corresponding author; e-mail: sgieral@ifpan.edu.pl

films at the nanometer scale, growth at low temperature, a high reproducibility of deposition and of uniformity over large substrates. These properties created ALD a perfect candidate for a low-cost deposition of various oxides for electronic and optoelectronic devices, as we demonstrated in the present work.

2. Experiment

The *n*-ZnO/*i*/*p*-GaN based heterojunction light emitting diodes were fabricated taking advantage of the ALD method [19]. The ALD oxide coatings were executed using the Savannah-100 reactor (Ultratech Company) by double-exchange chemical reactions. During sequential doses of metal and oxygen precursors separated by purging of neutral gas — nitrogen (called as one cycle in ALD system) thin oxide films were obtained. Precise thickness control can be easily achieved as a constant amount of layer material was deposited in each cycle, and film thickness was scaled by the number of ALD cycles. Thickness, growth temperature, length of precursors pulses (in milliseconds) and purging times were modified to ensure reproducibility and uniformity of grown oxides. Therefore, the length of one ALD cycle was 20 s. More details about optimization of the ALD process for oxide materials can be found in our previous works [17, 18]. Oxides (HfO_2, TiO_2, Al_2O_3, ZrO_2 and ZnO) were formed at low temperature (well below 300 °C) using tetrakis(dimethylamido)hafnium, trimethylaluminum, tetrakis(dimethylamido)zirconium, titaniumtetrachloride, and diethylzinc as metal precursors, deionized water as an oxygen precursor and GaN templates as substrates. The epitaxial *p*-GaN layers containing GaN:Mg/GaN:Mg/GaN/GaN:Si structures with thickness of 10/500/100/2000 nm were produced on the crystalline Al_2O_3 substrates in the TopGaN Company. Substrates were chemically cleaned before a growth processes. The use of *p*-type GaN and *n*-type ZnO semiconductors in optoelectronic devices required the development of metallic ohmic contacts which did not interfere with the concentration of carriers near metal/semiconductor interface. On ZnO and GaN surfaces there were evaporated ohmic contacts, consisting of metal layers of Ti and Au (10/40 nm thick Ti/Au) for ZnO, as well as Ni and Au (250/500 nm thick Ni/Au) for GaN. In addition, contacts for GaN were annealed at 500 °C for 10 min in a O_2 and N_2 atmosphere using the rapid thermal process.

The investigated *n-i-p* structures with oxide layers were characterized at a room temperature using a range of experimental methods. The structural characterization was performed by XRD, using the X'Pert Materials Research Diffractometer equipped with an X-ray mirror and a two-bounce monochromator at the incident beam. The diffracted beam was measured with a 2-dimensional solid-state X-ray detector (PIXcel). The layers thicknesses were measured on silicon substrates by the spectroscopic reflectometer (Nanocalc 2000). The surface morphology was investigated by atomic force microscopy (AFM, Bruker Dimension Icon) using the PeakForce Tapping and silicon nitride probes with sharp tips (tip radius — 2 nm). The surface roughness was determined by a root mean square (RMS) roughness of the AFM height measurements from images taken from a 10×10 μm^2 region. Optical spectra (photoluminescence, PL, and EL) of junction nanostructures have been characterized by the the Solar CM2203 spectrophotometer with a xenon lamp. The Hall effect measurements to determine the charge carrier concentration and mobility in layers were performed with a RH2035 system produced by PhysTech GmbH, with a permanent magnet giving a magnetic field of 0.426 T. The Hall measurements were done in the van der Pauw configuration with four contacts. Current–voltage (I–V) electrical characterizations for devices were performed using Keithley 2636A electrometers. I–V characteristics of the heterojunction determined the rectification ratio of the junction, defined as the ratio of forward to reverse currents (I_{on}/I_{off}). This ratio was mostly intent by a barrier height seen by electrons and holes.

3. Results and discussion

In this paper the properties of *n-i-p* diodes with oxide films deposited by the ALD method were analyzed. The schematic diagram of our *n*-ZnO/*i*/*p*-GaN heterostructure was shown in Fig. 1. The Hall measurements showed a stable hole conductivity of the magnesium-doped GaN films with the hole density of 4×10^{17} cm^{-3}, the mobility of 14 cm^2/(V s) corresponding to resistance of 1 Ω cm. These semiconductor layers with a smooth surface (RMS in range of 1–2 nm, see Fig. 2) were crystalline with a hexagonal wurtzite phase. On this substrate, the 5 nm thick interlayers consisting of one or two oxides such as HfO_2, Al_2O_3, ZrO_2, TiO_2, Al_2O_3/HfO_2, Al_2O_3/ZrO_2, TiO_2/ZrO_2 or TiO_2/HfO_2 were deposited at the low temperature in the ALD system. The growth rate of these oxides was in the range of 0.08–0.15 nm per cycle. The growth temperature was limited to 85 °C, taking into account the possibility of the deposition of high-k films with the required high dielectric constant of ≈ 40 for TiO_2, ≈ 23 for ZrO_2, ≈ 21 for HfO_2, and ≈ 10 for Al_2O_3) and suitable band gap resulting from wide energy gap (6.2 eV for HfO_2, 6.0 eV for ZrO_2, 3.9 eV for TiO_2 and 6.3 eV for Al_2O_3), atomically smooth surface with a RMS roughness below 1 nm as the intrinsic layers. Therefore, these films provided well-defined and free of additional defects and impurities interlayer/semiconductor interfaces as well as flat surface of semiconductors of optoelectronic devices. In conclusion, properly selected oxides minimized possible negative effects related to the mixing of materials near to the interface, which may decrease the reliability of electronic structures (see our previous work in Ref. [17]). Test measurements of *n-i-p* devices with Al_2O_3/HfO_2 interlayers clearly showed the advantageous properties of such a composite. Layers with the applied composition improved the surface morphology, performance and electric strength of the studied devices.

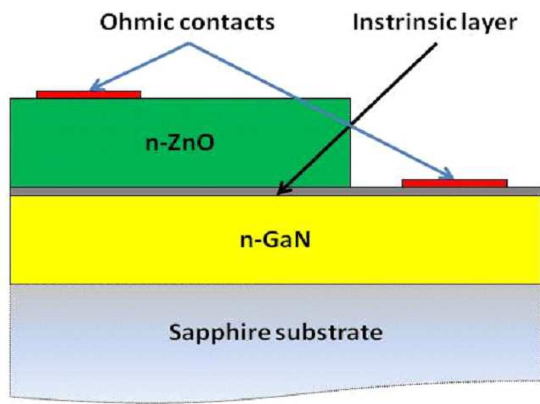

Fig. 1. Schematic diagram of the studied n-ZnO/intrinsic layer/p-GaN structure with ohmic metallic contacts obtained on sapphire substrate.

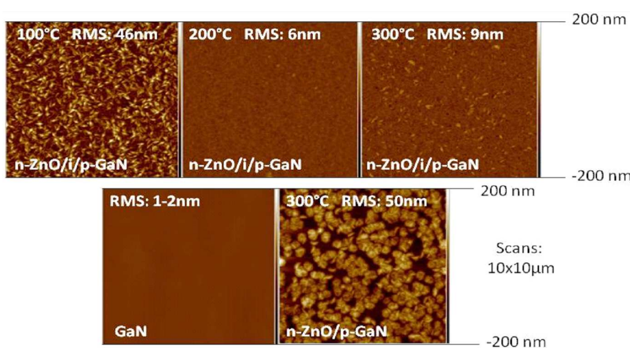

Fig. 2. AFM-studied top surface morphology of n-i-p and n-p heterostructures with ZnO grown at different temperatures and GaN layers obtained on sapphire substrate.

The p-GaN were used as semiconducting partner ZnO-based junctions. The n-ZnO layers were embedded in ALD processes at three temperatures of 100, 200 and 300 °C on the surfaces of $Al_2O_3/HfO_2/p$-GaN/Al_2O_3 structures and for comparison on p-GaN/Al_2O_3 structure. For the selected growth temperatures the growth rate of these oxides was 0.15, 0.14, and 0.10 nm per cycle, respectively. These zinc oxide films with thickness of about 800 nm were deposited in the form of hexagonal columns and had a wurtzite structure as indicated by the diffraction peaks (10.0), (00.2), (10.1), and (11.0) in the XRD spectrum. It has also been shown in previous work [20], the electrical properties of ALD zinc oxides can be controlled in a wide range, but thin polycrystalline layers exhibited the typical free electrons concentration of 5×10^{19} cm^{-3}, and their mobility reached a value about 20 cm^2/(V s), which corresponded to resistance value of 6×10^{-3} Ω cm. However, decrease of the growth temperature to 100 °C caused increase of electrical resistance of about 2×10^{-2} Ω cm by reducing of mobility and carriers concentration up to 5 cm^2/(V s) and 5×10^{18} cm^{-3}, respectively. Higher values of electrical resistances were determined by a large number of defects, grain scattering and/or increased surface roughness. The top surfaces of ZnO films (in n-i-p structures) grown at temperature of 100 °C were characterized by the surface roughness with RMS value at the level of 46 nm, as compared to the RMS values for ZnO grown at higher temperatures were below 10 nm, as was shown in Fig. 2.

The introducing of a thin wide band gap layer as interlayer between ZnO and GaN changed the properties of the optoelectronic device. The wide band energy of intrinsic layer in LED structure was necessary to obtain a required band offset of more than 1 eV in the conduction band for the n-ZnO semiconductor and less than 1 eV in the valence band for the p-GaN semiconductor. In consequence, the optimized intrinsic layer should block (reduce) the flow of electrons and facilitate the diffusion of holes in the junction structure [21]. This means that the interlayer in junction was desirable because the n-ZnO/p-GaN LED emitted mainly from the p-type GaN region and not from the n-type ZnO. The reason was as follows — electrons injection from n-type ZnO dominated over holes injection from p-type GaN, which was due to a much higher carriers concentration in n-type ZnO. The typical electroluminescence spectra of the n-ZnO/p-GaN device displayed emissions centered at 430–440 nm (mainly blue light) and weak emissions centred at 550 nm (violet and white light), while the homojunction GaN LEDs exhibited a max wavelength at 430 nm, due to the transition from conduction band edge to the Mg acceptor energy level in p-type side of the diodes [9, 22]. In addition, in this work investigated n-ZnO/p-GaN structures demonstrated the significantly rough surface with RMS value of 50 nm and relatively good electrical properties like the voltage operation from –4 to 4 V, low leakage current density at the level of 10^{-6} A for a voltage of –4 V, open voltage reaching a value below 1 V and rectification ratio $I_{\mathrm{on}}/I_{\mathrm{off}}$ in the range of 10^2–10^3 for 4 V with I_{on} 3 μA, as was shown in Figs. 1 and 3d.

Of analyzed wide band gap oxides, sufficient data exist to conclude that ALD oxides consisting of Al_2O_3/HfO_2 grown at low temperature were stable in contact with investigated semiconductor materials (see Refs. [17, 23]), which gave a suitable barrier to the flow of electrical charges from the semiconductor to the inside of the device. The Al_2O_3/HfO_2 very thin layer should be a good electron blocking and hole transporting layer for the p-GaN/n-ZnO LED because these dielectrics were a combination of high-k nature and the high conduction-band offset for Al_2O_3/ZnO interface was about 3 eV [24] and the relatively low valence-band offset for HfO_2/GaN interface was about 0.3 eV [25].

The interlayer improved the surface morphology which corresponds to performance and electrical properties of the n-ZnO/i/p-GaN heterostructures. The desirable, electrical properties of the LED devices such as the stable and wide voltage operation from –20 to 20 V, low leakage current density at the level of 10^{-9} A for a voltage of

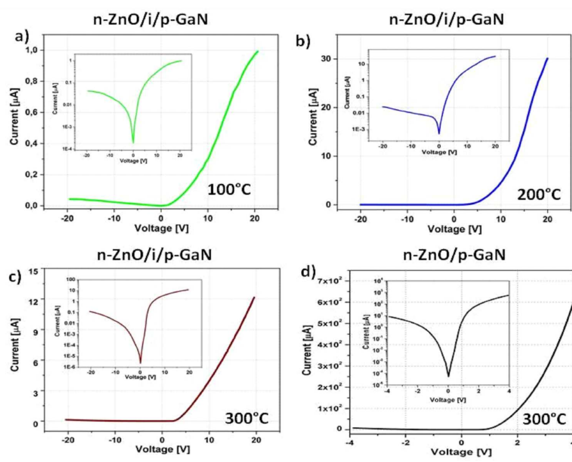

Fig. 3. *I–V* characteristic of: *n*-ZnO/*i*/*p*-GaN heterojunctions with ZnO layers obtained at (a) 100 °C, (b) 200 °C, (c) 300 °C, and (d) *n*-ZnO/*p*-GaN heterojunction with ZnO layer obtained at 300 °C (without intrinsic layer). For all structures there were performed ohmic contacts.

–20 V, open voltage reaching a value about 3 V and rectification ratio I_{on}/I_{off} in the range of 10^2–10^3 for 20 V were shown in Figs. 3a–c. These significant corrections of electrical parameters can be achieved by improving of quality of the morphological structures through lower defects and impurities in interlayer/semiconductor interfaces as well as flat surface of ZnO semiconductors which corresponds to increase of the surface smoothness of the *n*-ZnO/*i*/*p*-GaN structures to a value below 10 nm for heterojunction with ZnO layers grown at 200 and 300 °C and 40 nm for ZnO at 100 °C (see Fig. 1).

In Fig. 4 the EL spectra of the *n*-ZnO/*i*/*p*-GaN LED devices with ZnO films grown at different temperatures under different injection currents were presented. These EL spectra consisted of several bands in the visible range centered at about 385 and 405 nm (violet emission); 435, 475, and 495 nm (blue); 540 nm (green); and 585 nm (orange). The color coordinates were calculated using Gaussian fits of the EL spectra of the studied devices and demonstrated in a chromaticity diagram (CIE). The CIE diagram revealed that the *n*-ZnO/Al_2O_3/HfO_2/*p*-GaN LEDs can emit violet-blue, violet, blue-white and green-white light, which is demonstrated in Fig. 5. The white LEDs have been achieved for the heterostructures with ZnO layers grown at 300 °C, which showed the broad red-green luminescence with peak located from 430 to 750 nm and edge luminescence with peak concentrated at 380 nm (near UV) in the PL spectrum. The PL in these areas was characteristic for ZnO layers as shown in Refs. [26, 27]. The *n-i-p* devices containing ZnO layers grown at 100 °C also exhibited light emission in these both ranges, however, due to worse morphological and electrical parameters caused by more defects and impurities in layers [20]. These heterostructures emitted violet and violet-blue radiation. Instead, the LEDs containing ZnO layers deposited at 200 °C emitted only light in the violet color. The PL spectrum of these structures demonstrated the highest ratio of exciton-to-defect intensity, which explained such EL results. In this case, defect emission decreased and exciton emission dominated, which indicated that lower defects and impurities in ZnO layers grown at temperature of 200 °C.

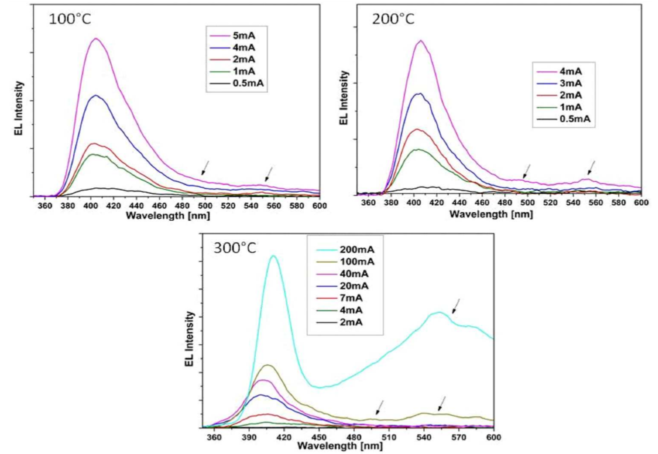

Fig. 4. EL spectra obtained for *n-i-p* LED heterostructures with ZnO deposited at 100, 200, and 300 °C under range injection current from 0.5 to 200 mA in the wavelength range from 350 to 600 nm.

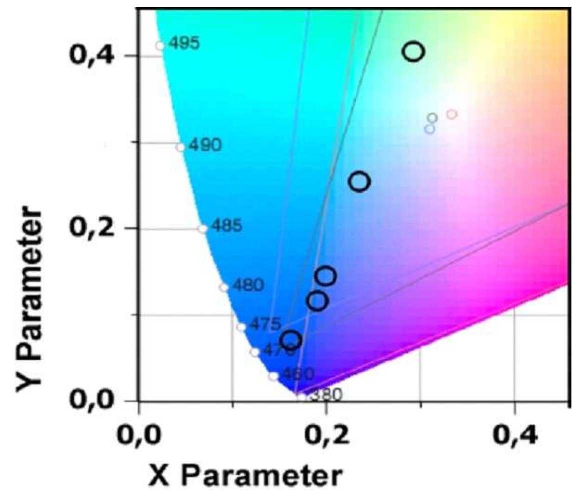

Fig. 5. CIE chromaticity diagram coordinates of *n*-ZnO/*i*/*p*-GaN LEDs with ZnO layer grown at 300 °C.

The obtained, in this work, white emission consisted of violet, blue, green, and orange-red radiation. The violet emission centered at in the ranges of 374–390 and 400–410 nm was attributed to the recombination processes observed in ZnO. The blue emission (425–445 nm) was associated with phenomena occurring in Mg-doped *p*-GaN layers. The defects presented in ZnO layers correspond to strong blue light (467–485 nm), blue-green (491–498 nm),

green (535–549 nm) and orange (565–589 nm). In conclusion, the white emission was related to the presence of impurities and defects in ZnO layers [12, 27].

4. Conclusion

In summary, we report the fabrication and characterization of LEDs based on n-ZnO/intrinsic layer/p-GaN heterojunctions. We investigated the influence of IL between n-ZnO and p-GaN on structural, electrical and optical properties of n-i-p heterostructures. Oxide-based devices were characterized by low reverse-leakage currents of about 10^{-9} A observed at room temperature, which was important in point of view of some electronic applications. The rectification ratio of our n-i-p junctions was $I_{\text{on}}/I_{\text{off}} = 10^2$–$10^3$ for the voltage of 20 V. The interlayer containing Al_2O_3/HfO_2 films was able to improve the performance of the n-ZnO/p-GaN heterojunction LEDs. These n-ZnO/i/p-GaN LEDs emit in violet-blue, violet, blue-white and green-white light. White emission can be observed without any extra-phosphors. The wide range of properties of the investigated oxides causes the versatility of ALD films as functional materials. The potential of these important materials can be used to increase the efficiency of oxide-based optoelectronic structures, while maintaining the cost of the device as low as possible, in contrast to LEDs, laser diodes based on n-GaN/p-GaN homojunction.

Acknowledgments

This work was supported by the National Science Centre (decision No. DEC-2013/09/N/ST5/00901).

References

[1] S.M. Sze, *Semiconductor Devices: Physics and Technology*, 3rd ed., Wiley, New York2012, Ch. 9.

[2] E.F. Schubert, *Light-Emitting Diodes*, 3rd ed., Rensselaer Polytechnic Institute Troy, New York 2018.

[3] F. Binet, J.Y. Duboz, N. Laurent, E. Rosencher, *J. Appl. Phys.* **81**, 6449 (1997).

[4] S. Nakamura, T. Mukai, M. Senoh, *Jpn. J. Appl. Phys.* **30**, L1998 (1991).

[5] S. Nakamura, *GaN Relat. Mater. 2*, 471 (1997).

[6] C. Klingshirn, *Phys. Status Solidi B* **244**, 3027 (2007).

[7] L.L. Chen, J.G. Lu, Z.Z. Ye, Y.M. Lin, B.H. Zhao, Y.M. Ye, J.S. Li, L.P. Zhu, *Appl. Phys. Lett.* **87**, 252106 (2005).

[8] X.L. Guo, Jae-Hyoung Choi, Hitoshi Tabata, Tomoji Kawai, *Jpn. J. Appl. Phys.* **40**, L177 (2001).

[9] Hao Zheng, Z.X. Mei, Z.Q. Zeng, Y.Z. Liu, L.W. Guo, J.F. Jia, Q.K. Xue, Z. Zhang, X.L. Du, *Thin Solid Films* **520**, 445 (2011).

[10] L. Wachnicki, S. Gieraltowska, B.S. Witkowski, S. Figge, D. Hommel, E. Guziewicz, M. Godlewski, *Acta Phys. Pol. A* **124**, 869 (2013).

[11] Y.I. Alivov, J.E. Van Nostrand, D.C. Look, M.V. Chukichev, B.M. Ataev, *Appl. Phys. Lett.* **83**, 2943 (2003).

[12] H. Huang, Guojia Fang, Songzhan Li, Hao Long, Xiaoming Mo, Haoning Wang, Yuan Li, Qike Jiang, D.L. Carroll, Jianbo Wang, Mingjun Wang, Xingzhong Zhao, *Appl. Phys. Lett.* **99**, 263502 (2011).

[13] C.H. Ahn, Young Yi Kim, Dong Chan Kim, Sanjay Kumar Mohanta, Hyung Koun Cho, *J. Appl. Phys.* **105**, 013502 (2009).

[14] J.B. You, X.W. Zhang, S.G. Zhang, J.X. Wang, Z.G. Yin, H.R. Tan, W.J. Zhang, P.K. Chu, B. Cui, A.M. Wowchak, A.M. Dabiran, P.P. Chow, *Appl. Phys. Lett.* **96**, 201102 (2010).

[15] H. Zhu, Chong–Xin Shan, Bin Yao, Bing–Hui Li, Ji–Ying Zhang, Zheng–Zhong Zhang, Dong–Xu Zhao, De–Zhen Shen, Xi–Wu Fan, You–Ming Lu, Zi–Kang Tang, *Adv. Mater.* **21**, 1613 (2009).

[16] S. Gieraltowska, L. Wachnicki, B.S. Witkowski, M. Godlewski, E. Guziewicz, *Opt. Appl.* **43**, 17 (2013).

[17] S. Gieraltowska, L. Wachnicki, B.S. Witkowski, R. Mroczynski, P. Dluzewski, M. Godlewski, *Thin Solid Films* **577**, 97 (2015).

[18] L. Wachnicki, T. Krajewski, G. Luka, B. Witkowski, B. Kowalski, K. Kopalko, J.Z. Domagala, M. Guziewicz, M. Godlewski, E. Guziewicz, *Thin Solid Films* **518**, 4556 (2010).

[19] M. Leskela, M. Ritala, *Thin Solid Films* **409**, 138 (2002).

[20] E. Guziewicz, M. Godlewski, L. Wachnicki, T.A. Krajewski, G. Luka, S. Gieraltowska, R. Jakiela, A. Stonert, W. Lisowski, M. Krawczyk, J.W. Sobczak, A. Jablonski, *Semicond. Sci. Technol. 27*, 074011 (2012).

[21] S.G. Zhang, X.W. Zhang, Z.G. Yin, J.X. Wang, J.J. Dong, Z.G. Wang, S. Qu, B. Cui, A.M. Wowchak, A.M. Dabiran, P.P. Chow, *J. Appl. Phys.* **109**, 093708 (2011).

[22] Shrawan Jha, Jin-Cheng Qian, Oleksandr Kutsay, Jaroslav Kovac Jr, Chun-Yan Luan, Juan Antonio Zapien, Wenjun Zhang, Shuit-Tong Lee, Igor Bello, *Nanotechnology* **22**, 245202 (2011).

[23] S. Gieraltowska, L. Wachnicki, B.S. Witkowski, E. Guziewicz, M. Godlewski, *Chem. Vap. Deposit.* **19**, 213 (2013).

[24] J.J. Robertson, *Vac. Sci. Technol. A* **31**, 050821 (2013).

[25] T.E. Cook, C.C. Fulton, W.J. Mecouch, K.M. Tracy, R.F. Davis, E.H. Hurt, G. Lucovsky, R.J. Nemanich, *J. Appl. Phys.* **93**, 3995 (2003).

[26] E. Przeździecka, L. Wachnicki, W. Paszkowicz, E. Lusakowska, T. Krajewski, G. Luka, E. Guziewicz, M. Godlewski, *Semicond. Sci. Technol.* **24**, 105014 (2009).

[27] A. Janotti, C.G. Van de Walle, *Phys. Rev. B* **76**, 165202 (2007).